Biophysical Chemistry 296 (2023) 106989

Contents lists available at ScienceDirect

Biophysical Chemistry

journal homepage: www.elsevier.com/locate/biophyschem

Composition of raft-like cell membrane microdomains resistant to styrene-maleic acid copolymer (SMA) solubilization

Karel Harant [a,d,*], Tomáš Čajka [b,*], Pavla Angelisová [c], Jana Pokorná [c], Václav Hořejší [c,*]

[a] Proteomics Core Facility, Faculty of Science, Charles University, BIOCEV, Prumyslova 595, Vestec CZ-25242, Czechia
[b] Institute of Physiology of the Czech Academy of Sciences, Vídeňská, 1083 142 20 Praha 4, Czechia
[c] Institute of Molecular Genetics of the Czech Academy of Sciences, Vídeňská, 1083 142 20 Praha 4, Czechia
[d] Institute for Environmental Studies, Faculty of Science, Charles University, Benatska 2, Prague 2 CZ-128 01, Czechia

ARTICLE INFO

Keywords:
Membrane rafts
SMA copolymer
Proteomics
Lipidomics
Jurkat cell line

ABSTRACT

An advantageous alternative to the use of detergents in biochemical studies on membrane proteins are the recently developed styrene-maleic acid (SMA) amphipathic copolymers. In our recent study [1] we demonstrated that using this approach, most T cell membrane proteins were fully solubilized (presumably in small nanodiscs), while two types of raft proteins, GPI-anchored proteins and Src family kinases, were mostly present in much larger (>250 nm) membrane fragments markedly enriched in typical raft lipids, cholesterol and lipids containing saturated fatty acid residues. In the present study we demonstrate that disintegration of membranes of several other cell types by means of SMA copolymer follows a similar pattern and we provide a detailed proteomic and lipidomic characterization of these SMA-resistant membrane fragments (SRMs).

1. Introduction

It is well established that cell membranes exhibit lateral heterogeneity – lipids and proteins form more or less dynamic micro/nano-domains of various size, specific lipids form lipid shells around transmembrane domains of proteins. An interesting and functionally important type of membrane micro/nano-domains are so called membrane rafts, which are enriched in cholesterol and lipids containing saturated fatty acid residues and selectively concentrate a specific set of mostly lipidated proteins and (glyco)lipids (recently reviewed in [2]). Traditionally, biochemical studies on membrane rafts were based mostly on their selective resistance to solubilization by some detergents. More recently, it has become obvious that the use of detergents may produce artifacts; therefore, detergent-resistant membrane fragments (DRMs) should not be considered equivalents of native rafts and the results based on DRMs should be interpreted with caution [3].

Styrene-maleic acid (SMA) amphipathic copolymers have recently emerged as an attractive alternative to the use of detergents. These copolymers cut the membrane into nanodiscs (often called SMA-lipid particles, SMALPs), which contain membrane proteins embedded in their relatively native lipid environment [4–6]. It has been demonstrated by biophysical studies that SMA molecules spontaneously insert into the membranes cutting them into “nanodiscs” of approx. 12 nm diameter. The phenyl moieties of the copolymer apparently intercalate between the lipid molecules, while the hydrophilic carboxy groups are exposed to the aqueous environment and may also interact with lipid extracellular polar headgroups [7]. The protein complexes associated with these SMALPs essentially behave like soluble (lipo)proteins, which can be studied using standard biochemical procedures.

In our recent study [1] we demonstrated that using membrane disintegration by means of the SMA copolymer, also most T cell membrane proteins were present in small nanodiscs. In contrast, two types of raft proteins, GPI-anchored proteins and Src family kinases, were mostly present in much larger (>250 nm) membrane fragments markedly enriched in typical raft lipids, cholesterol and lipids containing saturated fatty acid residues. These SMA-resistant membrane fragments (SRMs) were therefore similar to previously described DRMs. However, another type of presumably raft-associated proteins, namely palmitoylated transmembrane adaptor proteins LAT and PAG, previously demonstrated in DRMs, were essentially absent from the SRMs [1].

In the present study we aimed to determine, whether disintegration of membranes of several human cell types by means of the SMA copolymer follows a similar pattern. We examined whether such treatment more generally produces presumably raft-derived SRMs, and determined protein and lipid composition of these entities.

* Corresponding authors.
E-mail addresses: karel.harant@natur.cuni.cz (K. Harant), Tomas.Cajka@fgu.cas.cz (T. Čajka), vaclav.horejsi@img.cas.cz (V. Hořejší).

https://doi.org/10.1016/j.bpc.2023.106989
Received 7 September 2022; Received in revised form 21 February 2023; Accepted 28 February 2023
Available online 5 March 2023

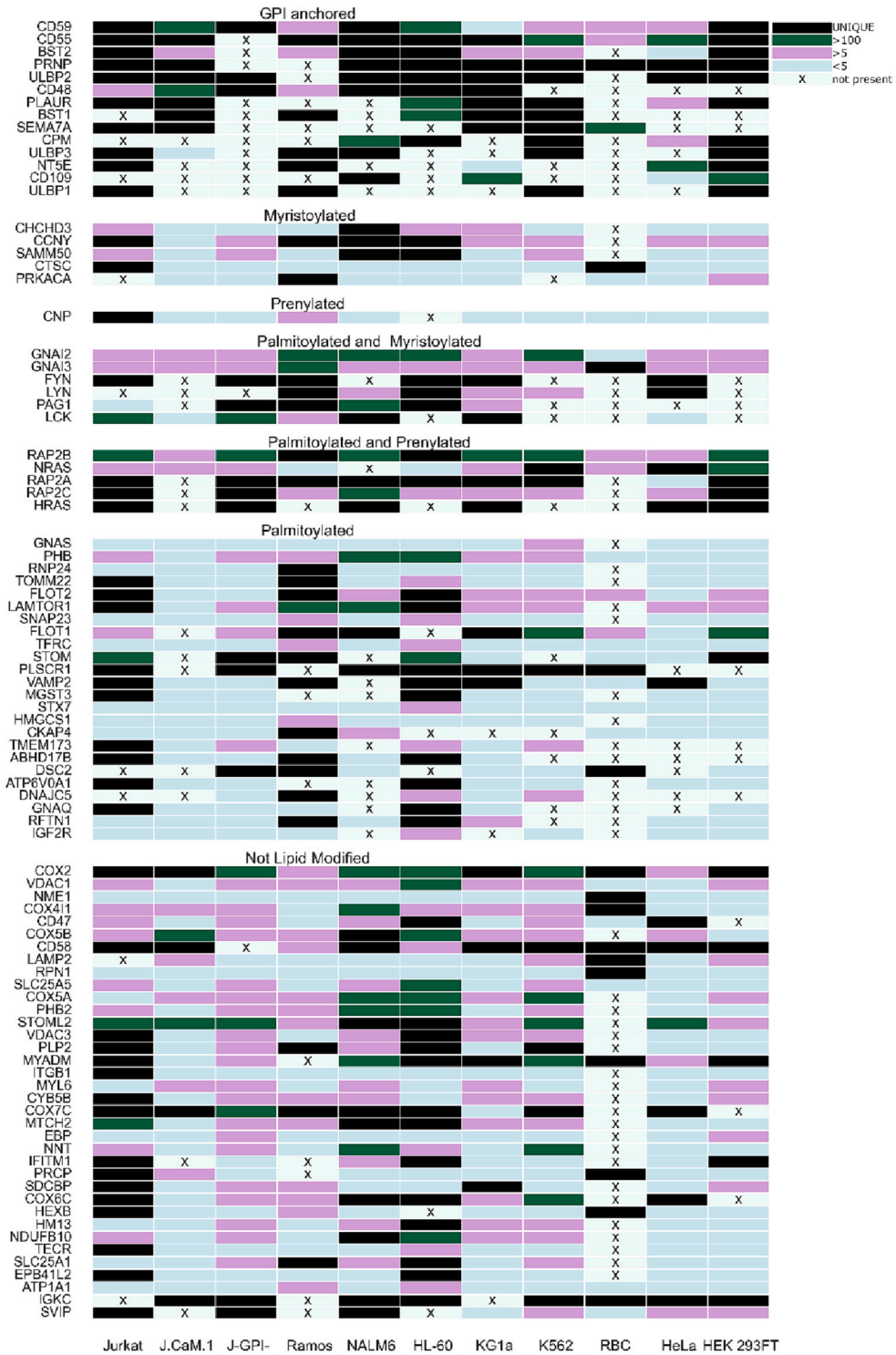

Fig. 1. Proteins selectively enriched in SRMs present in top fractions (1–5) of the density gradient. The samples were analyzed by mass spectrometry as described in detail in Experimental Procedures (2.7.). Membrane proteins with the intensity ratio "SRM fraction/whole cell lysate" more than twenty in at least one of the cell lines were selected, sorted according to the number of occurrences in the SRM fractions in all cell lines (regardless of the SRM/lysate intensity value) and proteins with occurrence in at least 7 cell types were included in this Figure. The selected proteins were clustered according to their predicted lipid modifications. The proteins were sorted according to their SRM/lysate ratio intensity values using the following color code: Black (unique in the SRM fraction); dark green (>100); pink (5 to 100); light blue (<5); light blue with X (missing both in the cell lysate and in the SRM fractions). The "unique" proteins of course must have been present also in the total cell lysates, but were obviously missed in these very complex protein-rich samples, while they were detectable in the less complex (less protein-rich) SRM fractions. The results are from single experiments for each cell line. (For interpretation of the references to color in this figure legend, the reader is referred to the web version of this article.)

2. Experimental procedures

2.1. Reagents

The following reagents were obtained from the indicated commercial sources: SMA sodium salt (Lipodisq™ Pre-Hydrolysed P (3:1 Ratio); m. w. 9,5 kDa; Malvern Pharmaceuticals), benzonase (Novagen), triethylammonium bicarbonate (TEAB; Pierce). Other common chemicals were from Sigma.

2.2. Cells and antibodies

Human cell lines Jurkat (T cell), Ramos (B cell), NALM-6 (pre-B cell), HL-60 (early myeloid), K562 (erythroid precursor), KG1a (early myeloid), HeLa (epithelial), HEK 293FT (embryonic kidney), were from the cell line collection of our Institute, Jurkat mutant cells J.CaM.1 (defective in Lck expression) was provided by Dr. A.Weiss, GPI-defective Jurkat mutant (J-GPI$^-$) by Dr. R. Schmidt; human erythrocytes (RBC) were obtained from local blood bank.

Rabbit polyclonal antibody to human CD59 was prepared previously

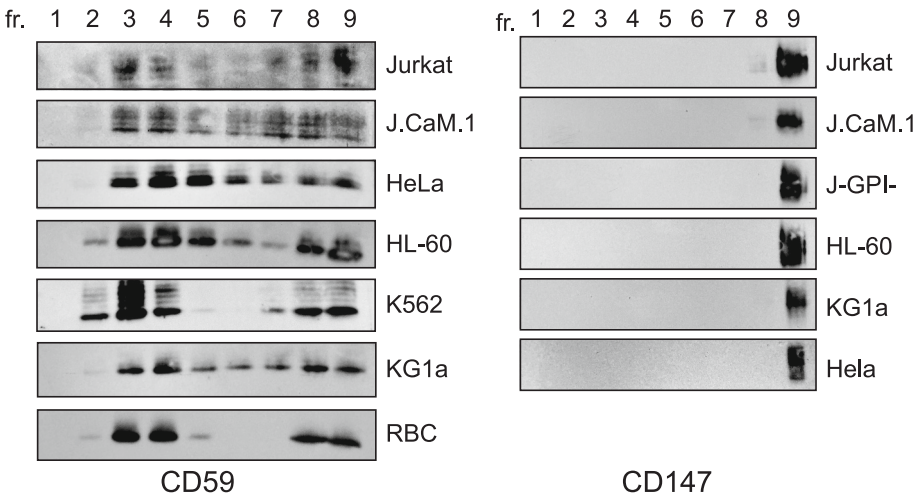

Fig. 2. Distribution of a membrane raft marker GPI-anchored glycoprotein CD59 (left panel) and a non-raft transmembrane glycoprotein CD147 (right panel) in the density gradient ultracentrifugation fractions. As described in paragraph 2.4., the indicated cell lines were solubilized by SMA, the lysates were fractionated by density gradient ultracentrifugation and the indicated proteins in the collected fractions were detected by Western blotting. Top fractions are No. 1. Only the relevant parts of the blots are shown, corresponding to the area around the m.w of the respective proteins (20 kDa for CD59 and 54 kDa for CD147). The results for cells negative in the respective proteins are not shown (CD59 in J-GPI-, Ramos, NALM-6, HEK 293FT; CD147 in Ramos, NALM-6, erythrocytes, K562, HEK 293FT). The materials corresponding presumably to membrane raft derived SRMs are present in the top fractions (mainly 2–5) based on their characteristic behavior during density gradient ultracentrifugation, as described in Experimental Procedures (2.4.). The reproducibility of the results was tested just for Jurkat cells – in total 6 similar experiments provided very similar results. Two experiments with very similar results were performed for HeLa, J.CaM.1 and KG1. The results for HL-60, K562 and erythrocytes (RBC) are from single experiments.

in our laboratory and is commercially available from EXBIO, mAb MEM-M6/1 (CD147) [8] was from EXBIO, goat anti-rabbit Ig-HRP and goat anti-mouse Ig-HRP from BioRad.

2.3. Cell and membrane solubilization

Cells (3×10^7) were solubilized for 1 h at room temperature in 1 mL of lysis buffer (20 mM Tris-HCl pH 8.2 containing 100 mM NaCl, Protease Inhibitor Cocktail III (Calbiochem), 10 mM EDTA, 50 mM NaF, 10 mM $Na_4P_2O_7$, and 1% SMA. 1 μL (25 U) of benzonase endonuclease solution and 10 μL of 1 M $MgCl_2$ was added to digest the viscous nuclear contents released by SMA. Such lysates were spun at 25,000 x*g* for 3 min. to remove remnants of nuclei and other insoluble materials, and used for gradient ultracentrifugation or for proteomic analysis. Erythrocyte membranes were obtained by centrifugation of human red blood cell hypotonic lysate and solubilized as described above (10 mg/mL), except that benzonase and $MgCl_2$ were omitted.

2.4. Density gradient ultracentrifugation

This method that has been previously used in studies that have dealt with presumably raft-derived DRMs [9] is suitable for the separation of relatively large and low-density membrane fragments (presumably rich in lipids) from small and/or relatively dense macromolecules and molecular complexes. For this type of separation, placing the sample at the bottom of the gradient is optimal. This separation was conducted as previously described [10]. Briefly, the SMA cell or erythrocyte membrane lysate (0.5 mL) was added to 0.5 mL of 80% (wt/vol) sucrose in lysis buffer and placed at the bottom of a 5.2 mL centrifuge tube. The mixture was then carefully overlaid with 1.8 mL of 30%, 0.8 mL 20%, 0.8 mL 10% and 0.7 mL 5% sucrose in lysis buffer and finally with 0.1 mL of lysis buffer. Centrifugation was performed at 10 °C in a Beckman Optima MAX-E ultracentrifuge, using a MLS50 swing-out rotor (21 h, 50,000 rpm). Nine 0.58 mL fractions were collected gradually from the top of the gradient. Proteins were then separated by SDS-PAGE and analyzed by immunoblotting.

2.5. Sedimentation of SMALPs by ultracentrifugation

As the protein concentrations in the SRMs containing top fractions of the density gradient were too low for proteomic analysis, SRMs present in the relevant gradient fractions (1–3, 4 + 5) were subjected to ultracentrifugation at 55,000 rpm (approx. 114,000 ×g) for 1 h at 18 °C using a TLA 110 rotor in a Beckman Optima ultracentrifuge. The sediments were used for proteomic and lipidomic analysis.

2.6. SDS-PAGE and Western blotting

SDS-PAGE (non-reduced boiled samples) and Western blotting were performed essentially as previously described [11]. The positions of the broadly expressed membrane raft marker, GPI-anchored protein CD59, and non-raft marker CD147 were visualized by Western blotting.

2.7. Proteomic analysis

LFQ MS analysis was performed as described previously [12]. Briefly, sedimented SMALPs (see section 2.5.) were dissolved in 100 mM TEAB with 1% sodium deoxycholate (SDC). Samples were digested with trypsin, and detergent was removed by liquid-liquid extraction [13]. Alternatively, samples of total cell lysates (see section 2.4.) mixed 1:1 with 2× SDS sample buffer were processed with Single-pot method [14].

Tryptic peptides were injected on a nano reverse-phase liquid chromatograph coupled with MS_core_Discoverer (nanoLC-MS) using a Thermo Orbitrap Fusion Mass spectrometer as described previously [12]. Briefly, peptides were separated and analyzed on an UltiMate 3000 RSLCnano system coupled to an Orbitrap Fusion Tribrid mass spectrometer (both from Thermo Scientific). Peptides were firstly loaded onto an Acclaim PepMap300 trap column (300 μm × 5 mm) packed with C18 (5 μm, 300 Å) in loading buffer (0.1% trifluoroacetic acid in 2% acetonitrile) for 4 min at 15 μL/min and then separated in an EASY-Spray column (75 μm × 50 cm) packed with C18 (2 μm, 100 Å, Thermo Scientific) at a flow rate of 300 nL/min. Mobile phase A (0.1% formic acid in water) and mobile phase B (0.1% formic acid in acetonitrile) were used to establish a 60-min gradient from 4% to 35% B. Eluted peptides were ionized by electrospray. A full MS spectrum (350–1400 *m/z* range) was acquired at a resolution of 120,000 at *m/z* 200 and a maximum ion accumulation time of 100 ms. Dynamic exclusion was set to 60 s. Higher-energy collisional dissociation (HCD) MS/MS spectra were acquired in iontrap in rapid mode and normalized collision energy was set to 30% with maximum ion accumulation time of 35 ms. An isolation width of 1.6 *m/z* units was used for MS^2.

Raw data were processed using MaxQuant version 2.0.2. [15].

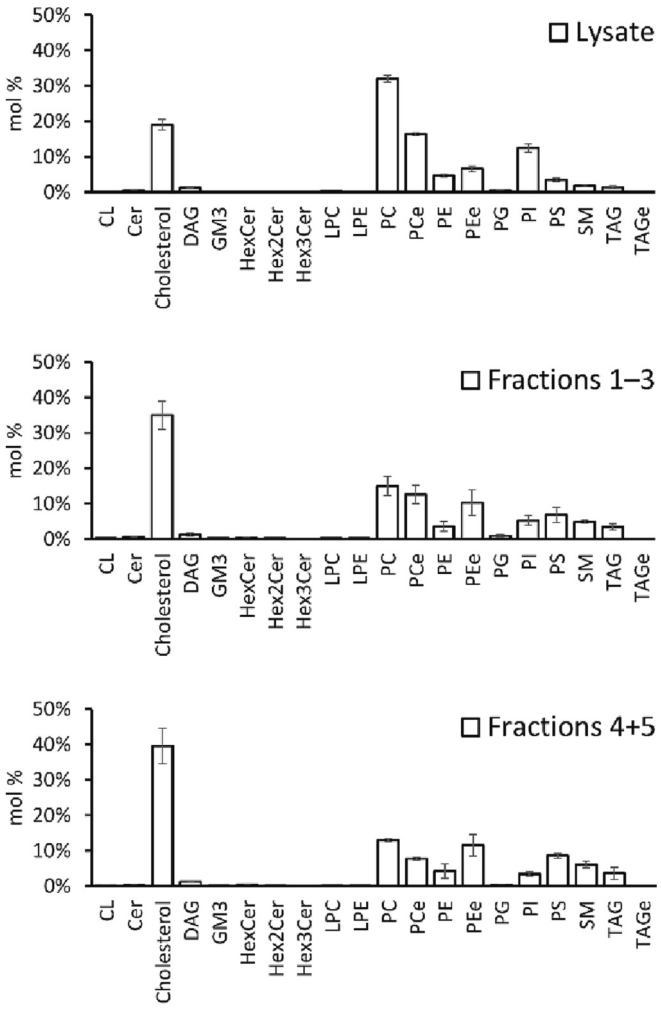

Fig. 3. Molar percentage distribution of lipid classes in whole Jurkat cell lysate and in the top density gradient fractions corresponding to the SRMs. Data from 3 independent experiments (standard deviations bars shown). Abbreviations: CL, cardiolipin; Cer, ceramide; DAG, diacylglycerol; GM3, ganglioside GM3; HexCer, hexosylceramide; Hex2Cer, dihexosylceramide; Hex3Cer, trihexosylceramide; LPC, lysophophatidylcholine; LPE, lysophosphatidylethanolamine; PC, phosphatidylcholine; PCe, ether-linked phosphatidylcholine; PE, phosphatidylethanolamine; PEe, ether-linked phosphatidylethanolamine; PG, phosphatidylglycerol; PI, phosphatidylinositol; PS, phosphatidylserine; SM, sphingomyelin; TAG, triacylglycerol; TAGe, ether-linked triacylglycerol.

Searches were performed using the human database from Uniprot (release 6/2021 entries). Trypsin cleaving specifity was used and two missed cleavages were allowed. The protein modifications were set as follows: cysteine (unimod nr: 39) as static and methionine oxidation (unimod: 1384) and protein N-terminus acetylation (unimod: 1) as variable. Search mass tolerances were used in MaxQuant default settings for Orbitrap and Iontrap. The precursor ion mass tolerance in the initial search was 20 ppm, the tolerance in the main search was 4.5 ppm, and the fragment ion mass tolerance was 0.5 Da. The false discovery rates for peptides and for proteins were set to 1%. Raw data and Maxquant serch is available on PRIDE repository [16], dataset: PXD031828.

Intensities of proteins were expressed as fractions of the total protein intensity. The ratio of these values was calculated for the total lysate of a given cell line and the corresponding SRM-containing sample. If this ratio was over 20 or a protein was unique for the SRM fractions in at least one cell line, the protein was considered as a membrane raft component. Proteins were annotated according to their membrane localization and possible lipid modifications. We consider four post-traslation modifications (palmitoylation, GPI-anchor, prenylation and myristoylation) as markers of membrane raft proteins [17–19]. Sources of protein modification annotation were as follows: palmitoylation (SwissPalm), GPI-anchor (UniProt annotation), prenylation (UniProt annotation), and myristoylation (MYR Predictor, Myristoylator). Although the data for SRMs containing fractions were measured separately for fractions 1–3 and 4 + 5, for the sake of simplicity they are here (Fig. 1, Table S1) presented as single samples, i.e. corresponding to pooled fractions 1–5. All identified proteins are listed in Supplementary Table 1, which contains the following sheets: (1) all identified proteins and their ratios between the total lysate and the SRM fractions, (2) list of proteins annotated as membrane ones, (3) list of proteins used for visualization in Fig. 1., (4) list of putative membrane raft proteins defined as above from their prevalence in the SRM fractions.

2.8. Lipid analysis

2.8.1. Sample preparation

A volume of 180 μL of cold methanol containing a mixture of lipid internal standards (CL 16:0/16:0/16:0/16:0, 221.0 pmol; Cer-NS d18:1/17:0, 49.9 pmol; Cholesterol-d7, 699.0 pmol; DAG 18:1/18:1-d5, 87.9 pmol; HexCer-NS 18:1/17:0, 38.5 pmol; LPC 17:1, 108.4 pmol; LPE 17:1, 147.8 pmol; PC 15:0/18:1-d7, 36.5 pmol; PE 17:0/17:0, 152.9 pmol; PG 17:0/17:0, 178.0 pmol; PI 15:0/18:1-d7, 65.0 pmol; PS 17:0/17:0, 3097.4 pmol; SM d18:1/17:0, 76.8 pmol; TAG 17:0/17:1/17:0-d5, 32.3 pmol) was added to the SRMs containing sediments (*see 2.5.*), followed by shaking (30 s) and sonication (3 pulses). Then, 600 μL cold methyl *tert*-butyl ether was added, followed by shaking (30 s), addition of 175 μL water, shaking (30 s), and centrifugation (16,000 rpm, 10 min, 4 °C). A volume of 300 μL of the upper organic phase was collected and evaporated. Dried lipid extracts were resuspended in 100 μL methanol containing the internal standard 12-[[(cyclohexylamino)carbonyl] amino]-dodecanoic acid (CUDA, 200 ng/mL); after shaking (30 s) and centrifugation (16,000 rpm, 5 min, 4 °C), the extracts were submitted to LC–MS analysis.

2.8.2. LC–MS analysis

The LC–MS system consisted of a Vanquish UHPLC System (Thermo Fisher Scientific, Bremen, Germany) coupled to a Q Exactive Plus mass spectrometer (Thermo Fisher Scientific). Details of LC–MS methods used for lipidomic profiling can be found elsewhere [20].

2.8.3. Data processing

MS-DIAL (v. 3.98) software program [21] was used for data processing. Lipids were annotated using accurate mass and MS/MS matching with LipidBlast library in MS-DIAL. In total, over 600 unique lipid species covering 20 lipid classes were annotated (Table S2). Quantification was performed using class-specific internal standards except for GM3, Hex2Cer and Hex3Cer species in which case internal standard HexCer-NS d18:1/17:0 was used. Results were expressed in pmol of particular lipid species per isolated membrane fraction followed by calculation of relative molar concentrations of particular lipid classes (%).

3. Results and discussion

3.1. Proteomic analysis

In our previous study [1] we demonstrated that following disintegration of cell membranes of a T cell line Jurkat or primary T cells by the SMA copolymer two types of membrane raft proteins, GPI-anchored proteins and Src family kinases, were mostly present in membrane fragments enriched in typical raft lipids, cholesterol and lipids containing saturated fatty acid residues. In contrast, the bulk of the membrane proteins and lipids were fully solubilized and apparently present

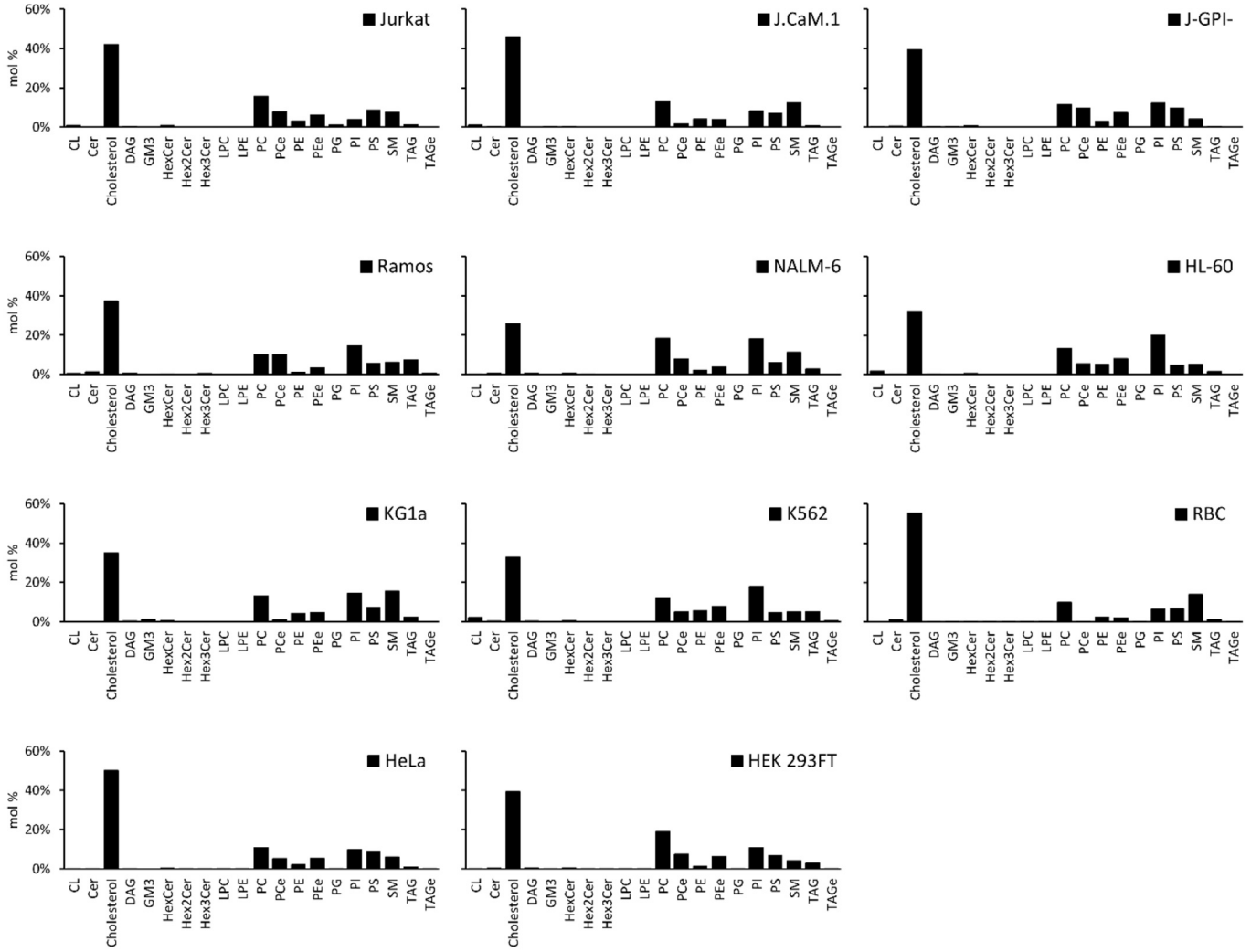

Fig. 4. a. **Molar percentage distribution of lipid classes in the density gradient fractions corresponding to the SRMs**. *As described above, for the sake of simplicity, only the data from the SRMs obtained from the pooled top gradient fractions 1–3 are shown; those from pooled fractions 4 + 5 had very similar lipid composition (not shown; the same holds for* Fig. 4b, c and d*).*

b. Molar percentage of total PC species based on the number (from 0 to 7) of double bonds (DB) in the SRM fractions.

c. Molar percentage of total PE species based on number (from 0 to 6) of double bonds (DB) in the SRM fractions.

d Molar percentage of total PI species based on number (from 0 to 6) of double bonds (DB) across fractions.

in small "nanodiscs".

We wondered whether membranes of other cell types also contain similar SMA-resistant patches (SRMs), and how they differ in their protein and lipid composition. Therefore, we examined in this respect human cell lines Jurkat (T cell, a positive control), Ramos (B cell), NALM-6 (pre-B cell), HL-60 (early myeloid), K562 (erythroid precursor), KG1a (early myeloid), HeLa (epithelial), HEK 293FT (embryonic kidney) and erythrocytes. Also, we included two relevant mutants of the Jurkat T cells - J.CaM.1 (defective in Lck expression) and GPI-defective Jurkat mutant (J-GPI^{-}), as we suspected that the absence of important raft components might affect the sensitivity to disintegration by SMA and composition of the SRMs.

The cells (or membranes, in the case of erythrocytes) were treated with 1% SMA as described above (2.3.), the resulting lysates were fractionated by sucrose gradient ultracentrifugation, the SRM fractions collected from the top part of the gradient (2.4.), concentrated by high-speed centrifugation (2.5.) and subjected to proteomic and lipidomic analysis.

As shown in Fig. 1 and Table S1, the buoyant SRMs (representing a small minority of total cell proteins [1]) from all cell types examined contained many lipid-modified (GPI, palmitoylated, myristoylated, prenylated) proteins. These included functionally important signaling membrane proteins such as Src family protein tyrosine kinases (Lck, Fyn, Lyn), G-proteins, as well as multiple extracellular GPI-anchored glycoproteins. Such membrane proteins apparently have affinity for the lipid environment rich in lipids with saturated hydrocarbon chains [2]. The proteins without lipid modifications may be targeted to SRMs either due to specific features of their transmembrane domains or via their associations with the lipidated ones. Actually, the SRMs contained many other lipid modified membrane proteins not shown in Fig. 1 (see Table S1).

It should be noted, that the SRMs examined here obviously originated not only from plasma membrane, but also from intracellular membrane compartments. Interestingly, there were also multiple mitochondrial proteins – their presence may not be surprising, as mitochondrial membrane raft-like membrane domains have been described before [22,23], as well as association of mitochondria with cell membranes [24].

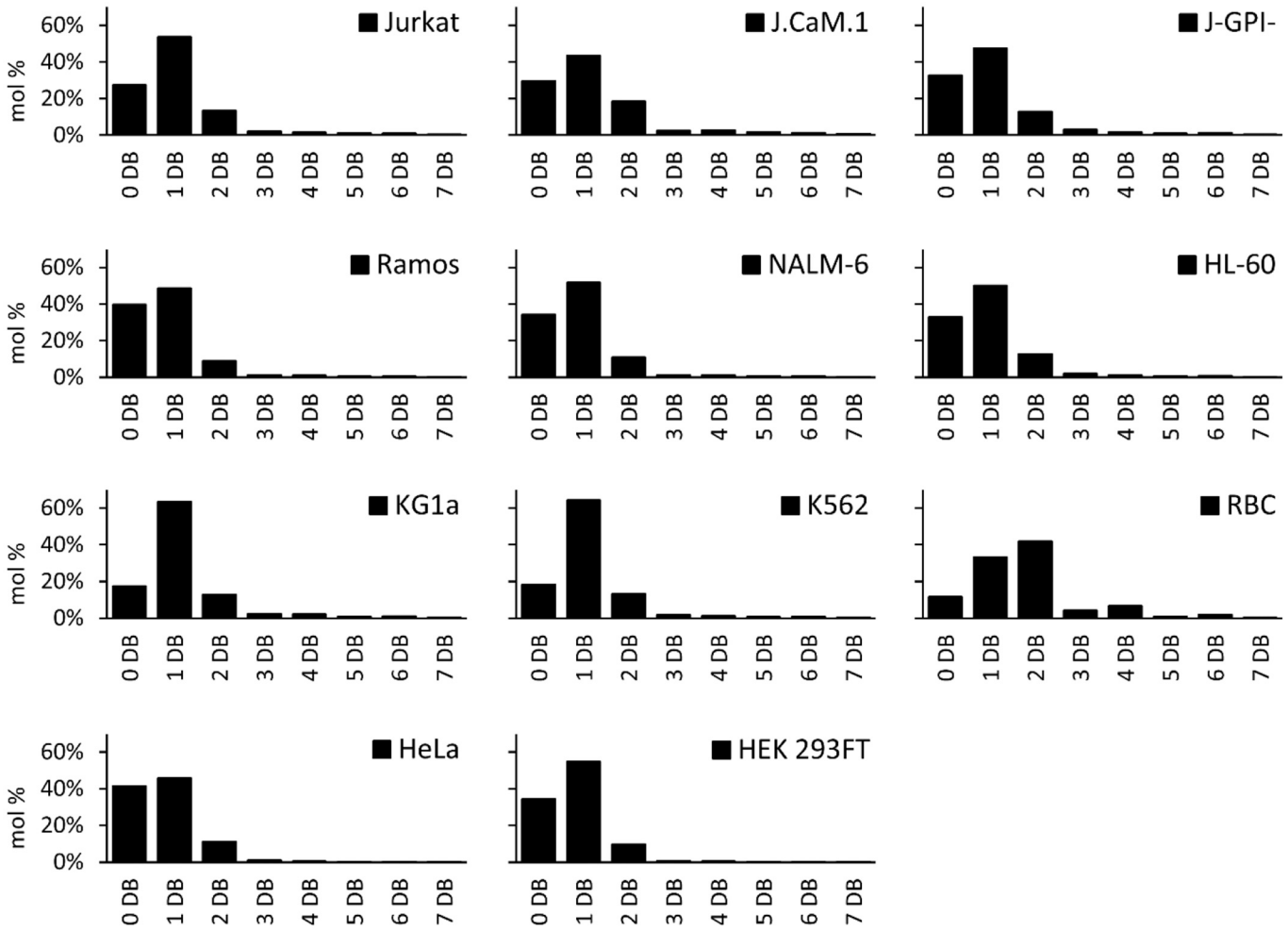

Fig. 4. (*continued*).

The distribution of a typical membrane raft marker (GPI-anchored protein CD59) in the density gradient ultracentrifugation fractions of several cell lines (Jurkat, J.CaM.1, HeLa, HL-60, K562, KG1a, erythrocyte) is illustrated by Western blotting (Fig. 2) and corresponds to our previous results with Jurkat cells (see Fig. 4 in [1]). As expected, a broadly expressed non-raft membrane protein CD147 was detected only in the bottom (non-raft) fractions of the gradient.

The membrane raft marker CD59 could not be detected by Western blotting in the cell lines Ramos, NALM-6, J-GPI$^-$ (not shown), although it was detectable in these cells by mass spectrometry (Fig. 1). It may be speculated that the antibody used in the Western blotting recognizes an epitope absent in the CD59 molecules expressed in some cell lines. The difference is especially intriguing in the case of the GPI-defective Jurkat cell mutant (J-GPI$^-$), which is correctly negative for several other GPI-anchored proteins in the proteomic analysis, but CD59 (and also ULBP2 and CD48) peptides are detectable in it (Fig. 1). In these cases, it is possible that the peptides detected by mass spectrometry are derived from intracellular precursors of these proteins, which failed to undergo the biosynthetic GPI-modification and lacked the epitope(s) recognized by the antibodies used in Western blotting. This surprising observation deserves further elucidation. The significance of the differences in the protein composition of the SRMs obtained from different cell lines are another point of interest for future studies. Especially the apparent differences between the WT Jurkat cells and the J.CaM.1 and J-GPI$^-$ mutants might be of interest, as both the mutant cell lines lack important raft components (tyrosine kinase Lck and GPI-anchored proteins, respectively) possibly involved in organization of membrane raft nanodomains.

3.2. Lipidomic analysis

First, we verified the reproducibility of the lipidomic analysis using the SRMs prepared in three separate experiments from the Jurkat cells (as described in paragraph 2.8). We analyzed separately the SRMs contained in the combined density gradient very top fractions 1–3 and those from combined fractions 4 and 5 and compared them with the lipid composition of whole cells. As shown in Fig. 3, the results were well reproducible and corresponded to the results of our previous study on T cell line Jurkat [1], i.e. significant differences between the whole cells and SRMs (especially markedly higher cholesterol content in the SRMs).

Then we performed lipidomic analysis of the SRMs obtained from all cell types examined (Fig. 4a – d). For the sake of simplicity, only the data from the SRMs obtained from the pooled top gradient fractions 1–3 are shown; those from pooled fractions 4 + 5 had very similar lipid composition (as shown for the Jurkat cells in Fig. 3). The data shown in Fig. 4a – d are from single experiments done under the same conditions as those shown in Fig. 3, which demonstrated good reproducibility.

As shown in Fig. 4a - d, the lipid composition of SRMs from all cell types examined was similar and corresponded to the results of our previous study on T cell line Jurkat, i.e. high cholesterol content and predominance of lipids with saturated fatty acid residues. Myeloid (HL-60, KG1a), erythroid (K562) and pre-B (NALM6) cell lines contained relatively more PIs than the other cells. The percentage of fully saturated PCs was markedly lower in KG1a, K562, and erythrocytes. Interestingly,

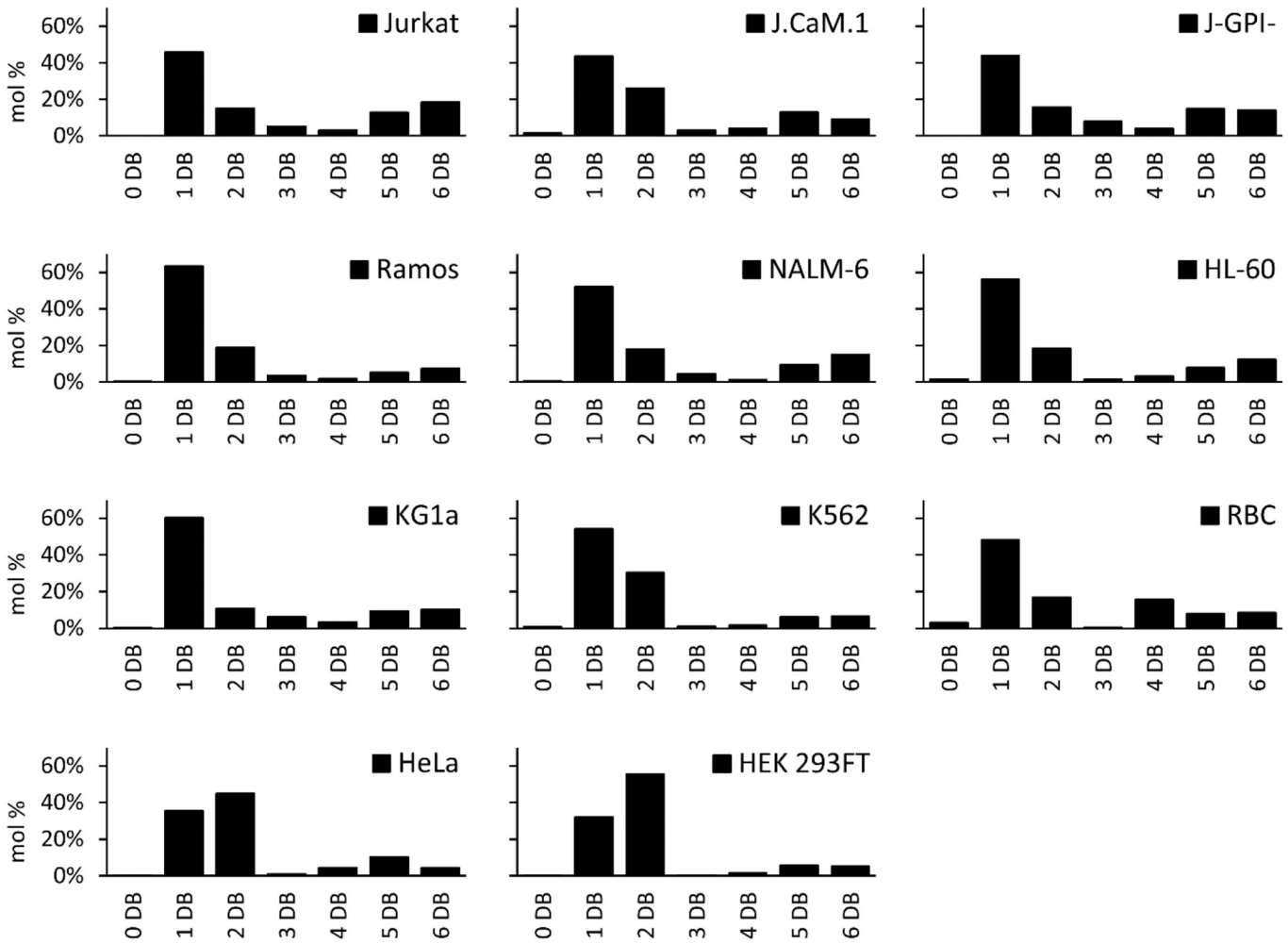

Fig. 4. (*continued*).

in contrast to phosphatidylcholine (PC), there were almost no fully saturated phosphatidylethanolamine (PE) and phosphatidylinositol (PI) lipid species.

It is presently not known what is the biological significance of these differences. As already noted above, the SRMs analyzed here obviously originated from both plasma membranes and intracellular ones, in a currently unknown ratio, which might have affected the observed differences in lipid (and protein) composition (mainly the distribution of various unsaturated species).

4. Conclusions

Our data demonstrate that all the examined cell types contain membrane regions resistant to disintegration by the SMA copolymer, specifically enriched by lipid-modified proteins and of similar lipid composition. This confirms and markedly extends our previous results on T cells [1] and may support the concept of membrane raft microdomains [2].

There has been a long and so far unfinished discussion concerning the relationship between membrane raft micro/nanodomains and the detergent-resistant fraction of membrane proteins (DRM). The present consensus is that the DRMs are not a faithful biochemical equivalent of native membrane rafts [25], as more recently thoroughly discussed by Sezgin et al [2] Importantly, as shown by us before [1] and in the present study, a similar phenomenon (existence of solubilization-resistant membrane fraction, SRM) is also observed when cell membranes are disintegrated by the SMA copolymer, which attacks membranes by a mechanism considerably different from detergents and produces very different major final products (SMALPs vs. detergent micelles). This may indicate that both these observations (existence of DRMs and SRMs) reflect an important non-artefactual feature of cell membranes. A reasonable hypothesis may be as follows. Upon exposure of cell membranes to certain detergents (such as Triton X-100) or to the SMA copolymer, bulk of the membrane is disintegrated into micelles or nanodiscs, respectively. Small native membrane raft nanodomains exhibiting (due to the nature of their lipid components) weak affinity toward these reagents, simply coalesce into larger aggregates that can be separated from the bulk of solubilized membrane proteins by standard biochemical methods and visualized by electron microscopy as 200–400 nm concave membrane sheets [1]. It is presently unclear to what extent the composition of the SRMs differs from that of the native raft micro/nanodomains, whether some of the protein or lipid components are lost (or added) during the SMA extraction. In this respect it should be noted that only a tiny fraction of total cell membrane proteins (<0.1%) is present in the SRMs, so the set of the proteins accumulated in the SRMs is highly specific.

SMA copolymer appears to be a significantly better alternative to detergents for cell membrane disintegration because it presumably preserves the more or less native lipid environment around the membrane proteins and the resulting nanodiscs and SRMs are apparently very stable even during prolonged incubation at physiological temperature [1]. We believe that various physiologically relevant cell treatments might result in specific compositional changes of the SRMs. This might serve as a potential useful tool of membrane biochemistry.

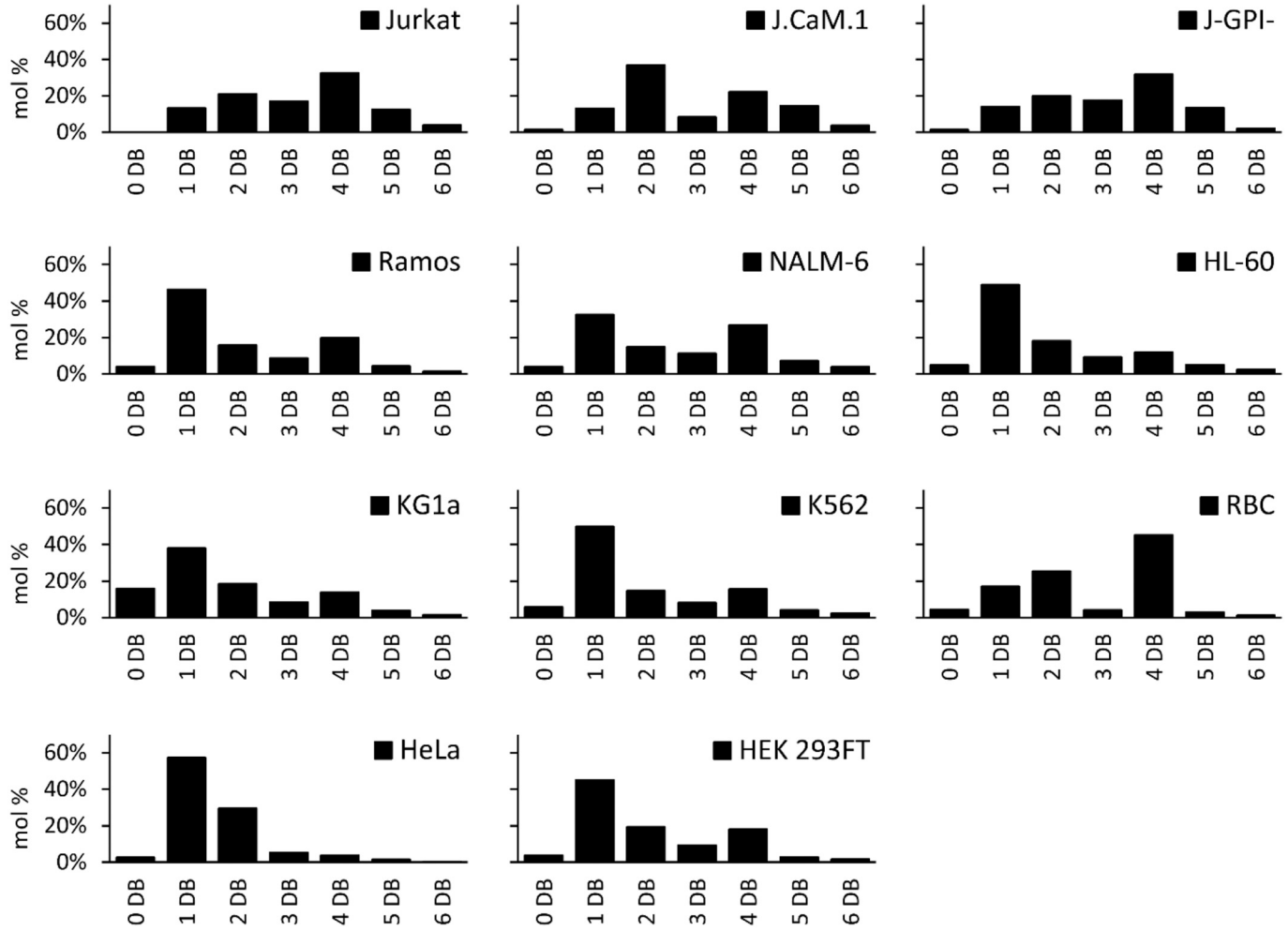

Fig. 4. (*continued*).

Furthermore, our current [26] and ongoing and so far unpublished studies indicate that additional types of membrane active copolymers produce alternative patterns of cell membrane disintegration and may thus provide a more nuanced biochemical insight into membrane organization. It should be noted that in the current literature there are only 3 studies dealing with some aspects of SRMs [1,27,28]. It seems likely that also a fraction of the protein-lipid complexes obtained by cell membrane disintegration by SMA or SMA derivatives, described in two other recent papers [29,30] are similar to the SRMs characterized in the present study.

Finally, there are several limitations of our study. First, we have not characterized the SRMs obtained from various cell lines as to their size; we assume that they may be comparable to those described in our previous study [1], i.e. in the order of a few hundreds of nanometers. Second, we have not studied the much smaller nanodiscs containing the majority of "fully solubilized" non-raft membrane proteins. Furthermore, we have to admit we just assume that the raft-derived proteins found in the SRMs reside in their truly native lipid environment. A rigorous proof of such an assumption would be very challenging. However, there are rather strong indications that transmembrane proteins present in the nanodiscs formed after membrane disintegration by SMA (much smaller than the SRMs) are present in a relatively native lipid environment, as reviewed e.g. in several recent papers [31–33].

Author contributions

V.H. and P.A. designed research, P.A. and J.P. performed the biochemical part of the study, K.H. and T.C. performed the proteomic and lipidomic analyses, respectively, V.H. wrote the manuscript that was edited by all authors.

Declaration of Competing Interest

The authors declare that they have no known competing financial interests or personal relationships that could have appeared to influence the work reported in this paper.

Data availability

Data will be made available on request.

Acknowledgements

The work was supported by Grant No. 19-04047S from the Czech Science Foundation and by the Institute of Molecular Genetics of the Czech Academy of Sciences (RVO 68378050). T.C. was supported by the Institute of Physiology of the Czech Academy of Sciences (RVO 67985823). Proteomics LCMS analyses were performed in Laboratory of Mass Spectrometry at BIOCEV research center; Faculty of Science, Charles University. The authors would like to acknowledge the Metabolomics Core Facility at the Institute of Physiology of the Czech Academy of Sciences for lipidomics profiling.

Appendix A. Supplementary data

Supplementary data to this article can be found online at https://doi.org/10.1016/j.bpc.2023.106989.

References

[1] P. Angelisova, O. Ballek, J. Sykora, O. Benada, T. Cajka, J. Pokorna, D. Pinkas, V. Horejsi, Biochim. Biophys. Acta Biomembr. 1861 (2019) 130.
[2] E. Sezgin, I. Levental, S. Mayor, C. Eggeling, Nat. Rev. Mol. Cell Biol. 18 (2017) 361.
[3] E. Sevcsik, G.J. Schutz, Bioessays 38 (2016) 129.
[4] T.J. Knowles, R. Finka, C. Smith, Y.P. Lin, T. Dafforn, M. Overduin, J. Am. Chem. Soc. 131 (2009) 7484.
[5] J.M. Dorr, S. Scheidelaar, M.C. Koorengevel, J.J. Dominguez, M. Schafer, C.A. van Walree, J.A. Killian, Eur. Biophys. J. 45 (2016) 3.
[6] M. Overduin, C. Trieber, R.S. Prosser, L.P. Picard, J.G. Sheff, Membranes (Basel) (2021) 11.
[7] M. Jamshad, V. Grimard, I. Idini, T.J. Knowles, M.R. Dowle, N. Schofield, P. Sridhar, Y.P. Lin, R. Finka, M. Wheatley, O.R. Thomas, R.E. Palmer, M. Overduin, C. Govaerts, J.M. Ruysschaert, K.J. Edler, T.R. Dafforn, Nano Res. 8 (2015) 774.
[8] C. Koch, G. Staffler, R. Huttinger, I. Hilgert, E. Prager, J. Cerny, P. Steinlein, O. Majdic, V. Horejsi, H. Stockinger, Int. Immunol. 11 (1999) 777.
[9] D.A. Brown, J.K. Rose, Cell 68 (1992) 533.
[10] P. Otahal, P. Angelisova, M. Hrdinka, T. Brdicka, P. Novak, K. Drbal, V. Horejsi, J. Immunol. 184 (2010) 3689.
[11] T. Brdicka, D. Pavlistova, A. Leo, E. Bruyns, V. Korinek, P. Angelisova, J. Scherer, A. Shevchenko, I. Hilgert, J. Cerny, K. Drbal, Y. Kuramitsu, B. Kornacker, V. Horejsi, B. Schraven, J. Exp. Med. 191 (2000) 1591.
[12] J. Stafkova, P. Rada, D. Meloni, V. Zarsky, T. Smutna, N. Zimmann, K. Harant, P. Pompach, I. Hrdy, J. Tachezy, Mol. Cell. Proteomics 17 (2018) 304.
[13] T. Masuda, M. Tomita, Y. Ishihama, J. Proteome Res. 7 (2008) 731.
[14] C.S. Hughes, S. Moggridge, T. Muller, P.H. Sorensen, G.B. Morin, J. Krijgsveld, Nat. Protoc. 14 (2019) 68.
[15] J. Cox, M.Y. Hein, C.A. Luber, I. Paron, N. Nagaraj, M. Mann, Mol. Cell. Proteomics 13 (2014) 2513.
[16] Y. Perez-Riverol, A. Csordas, J. Bai, M. Bernal-Llinares, S. Hewapathirana, D. J. Kundu, A. Inuganti, J. Griss, G. Mayer, M. Eisenacher, E. Perez, J. Uszkoreit, J. Pfeuffer, T. Sachsenberg, S. Yilmaz, S. Tiwary, J. Cox, E. Audain, M. Walzer, A. F. Jarnuczak, T. Ternent, A. Brazma, J.A. Vizcaino, Nucleic Acids Res. 47 (2019) D442.
[17] K.A. Melkonian, A.G. Ostermeyer, J.Z. Chen, M.G. Roth, D.A. Brown, J. Biol. Chem. 274 (1999) 3910.
[18] I. Levental, M. Grzybek, K. Simons, Biochemistry 49 (2010) 6305.
[19] D. Yurtsever, J.H. Lorent, J. Phys. Chem. B 124 (2020) 7574.
[20] G. Sistilli, V. Kalendova, T. Cajka, I. Irodenko, K. Bardova, M. Oseeva, P. Zacek, P. Kroupova, O. Horakova, K. Lackner, A. Gastaldelli, O. Kuda, J. Kopecky, M. Rossmeisl, Nutrients (2021) 13.
[21] H. Tsugawa, T. Cajka, T. Kind, Y. Ma, B. Higgins, K. Ikeda, M. Kanazawa, J. VanderGheynst, O. Fiehn, M. Arita, Nat. Methods 12 (2015) 523.
[22] M. Sorice, V. Manganelli, P. Matarrese, A. Tinari, R. Misasi, W. Malorni, T. Garofalo, FEBS Lett. 583 (2009) 2447.
[23] L. Ciarlo, V. Manganelli, T. Garofalo, P. Matarrese, A. Tinari, R. Misasi, W. Malorni, M. Sorice, SO - Cell Death Differ, PMID- 20053954 OWN - NLM STAT- Publisher, 2010 Jan 15.
[24] S. Missiroli, S. Patergnani, N. Caroccia, G. Pedriali, M. Perrone, M. Previati, M. R. Wieckowski, C. Giorgi, Cell Death Dis. 9 (2018) 329.
[25] D. Lichtenberg, F.M. Goni, H. Heerklotz, Trends Biochem. Sci. 30 (2005) 430.
[26] M. Janata, E. Cadova, P. Angelisova, T. Charnavets, V. Horejsi, V. Raus, Macromol. Biosci. 22 (2022), e2200284.
[27] D.J.K. Swainsbury, S. Scheidelaar, N. Foster, R. van Grondelle, J.A. Killian, M. R. Jones, Biochim. Biophys. Acta Biomembr. 1859 (2017) 2133.
[28] J.J. Dominguez Pardo, J.M. Dorr, A. Iyer, R.C. Cox, S. Scheidelaar, M. C. Koorengevel, V. Subramaniam, J.A. Killian, Eur. Biophys. J. 46 (2017) 91.
[29] A.J. Smith, K.E. Wright, S.P. Muench, S. Schumann, A. Whitehouse, K.E. Porter, J. Colyer, Sci. Rep. 9 (2019) 16408.
[30] M. Esmaili, B.P. Tancowny, X. Wang, A. Moses, L.M. Cortez, V.L. Sim, H. Wille, M. Overduin, J. Biol. Chem. 295 (2020) 8460.
[31] J.F. Bada Juarez, A.J. Harper, P.J. Judge, S.R. Tonge, A. Watts, Chem. Phys. Lipids 221 (2019) 167.
[32] C.J. Brown, C. Trieber, M. Overduin, Curr. Opin. Struct. Biol. 69 (2021) 70.
[33] M. Overduin, M. Esmaili, Chem. Phys. Lipids 218 (2019) 73.